Open Archive Toulouse Archive Ouverte (OATAO)

OATAO is an open access repository that collects the work of Toulouse researchers and makes it freely available over the web where possible

This is an author's version published in: **http://oatao.univ-toulouse.fr/21053**

Efficiency of plasma elaborated sub-stoichiometric titanium oxide (Ti$_4$O$_7$) ceramic electrode for advanced electrochemical degradation of paracetamol in different electrolyte media

Soliu O. Ganiyu[a], Nihal Oturan[a,*], Stéphane Raffy[b], Marc Cretin[c], Cristel Causserand[d], Mehmet A. Oturan[a]

[a] *Université Paris-Est, Laboratoire Géomatériaux et Environnement (EA 4508), UPEM, 77454 Marne-la-Vallée, France*
[b] *Saint-Gobain C.R.E.E., 550 Avenue Alphonse Jauffret, 84300 Cavaillon, France*
[c] *IEM (Institut Européen des Membranes), UMR 5635 (CNRS-ENSCM-UM), Université de Montpellier Place E. Bataillon, F-34095 Montpellier, Cedex 5, France*
[d] *Laboratoire de Génie Chimique, Université de Toulouse, CNRS, INPT, UPS, Toulouse, France*

A B S T R A C T

This paper investigates the behavior of conductive Ti$_4$O$_7$ ceramic anode in different electrolytes during the degradation of the anti-inflammatory drug paracetamol (PCM) by advanced electrochemical oxidation processes mainly anodic oxidation with generation of H$_2$O$_2$ (AO-H$_2$O$_2$) and electro-Fenton (EF). Regardless of the medium, better degradation and mineralization efficiency was always observed with EF compared to AO-H$_2$O$_2$. The degradation of PCM was carried out by hydroxyl radical ($^{\bullet}$OH) produced on the anode surface from water oxidation and mediated oxidation in the solution from oxidant species generated at the anode such as sulfate radicals and active chlorine species depending on the supporting electrolytes used, as well as $^{\bullet}$OH generated homogeneously in the solution by electrochemically assisted Fenton's reaction. Faster degradation was observed in Cl$^-$ compared to other media, but the solution was poorly mineralized. Highest total organic (TOC) removal efficiency with excellent degradation rate was attained in SO$_4$$^{2-}$ with either process, thus remain the best medium for advanced electrochemical wastewater treatment. Comparative studies with dimensional stable anode (DSA) and boron-doped diamond anode (BDD) showed similar trend of degradation and TOC removal efficiency with DSA anode achieving low mineralization power compared to Ti$_4$O$_7$ anode, whereas BDD showed slightly better efficiency than Ti$_4$O$_7$ in all electrolytes studied. The analysis of concentration of generated active chlorine species, especially ClO$^-$, during AO-H$_2$O$_2$ decreased in the order: DSA > Ti$_4$O$_7$ > BDD. Therefore, the Ti$_4$O$_7$ electrode was found to be a promising anode material for an efficient treatment of PCM in SO$_4$$^{2-}$, NO$_3$$^-$ and ClO$_4$$^-$ media but less effective in Cl$^-$ medium.

1. Introduction

Electrochemical advanced oxidation processes (EAOPs) as an alternative treatment technique for organic-contaminated wastewater has been extensively developed and studied in the last two decades due to their versatility, environmental compatibility, high energy efficiency and amenability to automation [1–4]. The oxidative degradation and efficient removal of organic pollutant in EAOPs is achieved by means of in-situ generated hydroxyl radical ($^{\bullet}$OH), which is a very reactive non-selective reagent and strong oxidant (second strongest oxidant known after fluorine) [5–8]. Among EAOPs, anodic oxidation (AO) and electro-Fenton (EF) processes in which $^{\bullet}$OH are generated either at the surface of the high-oxygen overpotential anode (M) via water oxidation (Eq.

(1)) and/or in the bulk through electrochemically assisted Fenton reaction (Eq. (2)) are the most widely studied processes due to their excellent efficiency and ease of operation [1,3,5,9,10].

$$M + H_2O \rightarrow M(^{\bullet}OH) + H^+ + e^- \tag{1}$$

$$Fe^{2+} + H_2O_2 + H^+ \rightarrow Fe^{3+} + {}^{\bullet}OH + H_2O \tag{2}$$

Additionally, when treated solution containing high concentration of chloride ions (i.e. reverse osmosis concentrate), active chlorine species such as Cl$_2$, HClO and ClO$^-$, are generated (Eqs. (3–5)) (depending on the pH of the solution) in parallel with $^{\bullet}$OH and/or M($^{\bullet}$OH) and can involve in the degradation of organic pollutants [5,8,11,12]. However, this action is often accompanied by the formation of highly toxic

chloramines, trihalomethanes, and haloacetic acids as well as refractory organochlorinated intermediates that are very toxic and difficult to mineralize [13–15]. This implies that the type of oxidants generated during electrochemical treatments and in turn, the efficiency of process is strongly influence by the medium/electrolyte in which the treatment is being carried out.

$$2Cl^- \rightarrow Cl_{2(aq)} + 2e^- \tag{3}$$

$$Cl_{2(aq)} + H_2O \rightarrow HClO + Cl^- + H^+ \tag{4}$$

$$HClO \leftrightarrow ClO^- + H^+ \tag{5}$$
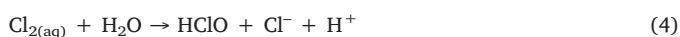
Ceramic electrode based on sub-stoichiometric TiO_2 developed in 80's for application as electrodes in batteries, sensors and corrosion protection has recently been investigated as an alternative low-cost anode material for possible application in electrochemical wastewater treatment [16–22]. The structural, electrical, electrochemical as well as corrosion behavior of bare and coated electrodes made from these material are available in literature [16,23–25]. They are majorly prepared by reduction of stoichiometric TiO_2, which is one of the most abundant feedstock on the planet [18,26]. Studies have shown that the sub-stoichiometric TiO_2 such as Ti_4O_7 behave as "non-active" anode as it have a large O_2 evolution overvoltage, can generate weakly adsorbed $\cdot OH$ (M(OH)) from water oxidation and therefore achieve high mineralization of organic pollutants [16,27,28]. Their electrochemical oxidation ability is significantly better than that of active anodes like DSA or Pt but slightly lower than that of BDD anode [16]. Most studies that have been conducted with sub-stoichiometric TiO_2 for electrochemical wastewater treatment application including the recent studies from our group, were carried out in sulfate medium [19,20,26,28]. Therefore, there is need for investigating the performance behavior of this electrode in other media such as chloride, nitrate and chlorate in order to understand its efficiency and suitability for electrochemical wastewater treatment.

Paracetamol (PCM), also known as acetaminophen or *N*-(*p*-hydroxyphenyl)-acetamide, is one of the most frequently used drugs worldwide, and has been found in sewage effluents at concentration up to 6.0–10 µg L^{-1} [29,30]. Contamination from manufacturing wastes/site may also be the source of this compound in environment and its detection is greater in urban centers where huge quantities of the drug usage are expected [31]. Although, the adverse health effects of low amounts of pharmaceuticals in natural water bodies has not been well proven, there are grown concern about their possible toxicity and health implications due to their fast distribution and accumulation in environment [32–34]. Their accumulation in aquatic environment is majorly due to inadequacy of the treatment techniques currently applied in wastewater treatment plants, which can only achieve partial destruction of the pollutants [8,35,36].

Advanced oxidation processes such as ozonation, UV-peroxidation (UV/H$_2$O$_2$) and Fe^{2+}, Cu^{2+} and UV catalyzed ozonation have been reported to achieve partial mineralization of PCM solution [36,37]. EAOPs such as AO, EF and photo electro-Fenton have also been studied for the removal of PCM with poor mineralization efficiency reported for AO with commercial electrodes such as Pt, Ti/SnO$_2$, Ebonex® and Ti/IrO$_2$, whereas excellent mineralization (> 80% TOC removal) was achieved with BDD anode and Fenton-based EAOPs [19,35,38–40].

In this paper, we investigated the electrochemical oxidation potential of sub-stoichiometric TiO_2 for degradation and mineralization of acidic solution of PCM in different electrolyte media. The Ti_4O_7 electrode was prepared by reduction of commercial TiO_2 in an electric arc furnace, followed by high temperature (10 000–15 000 °C) plasma deposition on Ti-alloy substrate. The structural properties of this electrode has been reported elsewhere [20]. This production technique is cost-efficient because plasma technology is a widely accepted technique for coating large surface, up to 1 m^2 or even more, thus economical for commercial production than CVD used in BDD anode production. The influence of the EAOPs types (i.e. AO with H$_2$O$_2$ generation (AO-H$_2$O$_2$) and EF) and current on the degradation kinetics of PCM and mineralization rate of its aqueous solution was carefully examined. For comparison, similar studies were performed with commercial DSA and BDD anodes. The generated short-chain carboxylic acids, the inorganic ions released in the treated solution and the aromatic intermediate formed during the electrochemical oxidation of PCM in sulfate medium were identified and/or quantified and a plausible reaction sequence for complete mineralization of PCM by hydroxyl radicals was proposed.

2. Experimental procedures

2.1. Chemicals

Reagent grade PCM (C$_8$H$_9$NO$_2$ – purity > 98%) was purchased from Sigma-Aldrich and used without further purification. Anhydrous sodium sulfate (Na$_2$SO$_4$), sodium chloride (NaCl), sodium nitrate (NaNO$_3$) and sodium chlorate (NaClO$_4$) used as supporting electrolyte were of reagent grade supplied by Merck and Acros Organics. All the solutions were prepared with high-purity water obtained from a Millipore Milli-Q system with resistivity > 18 MΩ cm at a room temperature (23 ± 2 °C). Organic solvents and other chemicals used were either of HPLC or analytical grade purchased from Merck, Fluka and Sigma-Aldrich.

2.2. Electrochemical cell

All electrolyses were performed in an open and undivided cylindrical reactor of 250 mL capacity in which the aqueous solutions of PCM were placed. Three electrodes, all with 24 cm^2 (4 cm × 6 cm) surface area, were used as anode: Ti$_4$O$_7$ (thin film deposited on Ti alloy from Saint-Gobain CREE, France), commercial DSA (a mixed metal oxide Ti/RuO$_2$-IrO$_2$ from Baoji Xinyu GuangJiDian Limited Liability Company, China) and BDD (thin-film deposited on a niobium substrate from CONDIAS, Germany). The cathode was a tri-dimensional, large surface area carbon-felt (14 cm × 5 cm × 0.5 cm (in width)), from Carbone-Lorrain, France.

In all trials, the anode was centered in the electrochemical cell and surrounded by the cathode (carbon-felt), covering the inner wall of the cell. $\cdot H_2O_2$ was continuously generated *in situ* by 2 e$^-$ reduction of dissolved O$_2$ at the carbon felt cathode. The concentration of O$_2$ in the solution was maintained constant by continuously bubbling compressed air via a silica frit at about 1 L min^{-1}, starting 10 min prior to electrolyses. All trials were performed with 230 mL aqueous solutions of 0.2 mM PCM (corresponding to 19.2 mg L^{-1} TOC) in 0.05 M Na$_2$SO$_4$ or 0.1 M NaCl, NaNO$_3$ or NaClO$_4$ as supporting electrolyte, at room temperature (23 ± 2 °C).

2.3. Instrument and analytical procedures

The electrolyses were performed with a Hameg HM8040 triple power supply at constant current. A CyberScan pH 1500 pH-meter (Eutech Instruments) was employed to measure solution pH. The mineralization of the treated solutions were analyzed from the decay of the dissolved organic carbon, which can be considered as the total organic carbon (TOC) in the case of highly water-soluble organic compounds like PCM. A Shimadzu VCSH TOC analyzer was used to determine TOC in accordance with the thermal catalytic oxidation principle. Reproducible TOC values, within ± 2% accuracy were found using the non-purgeable organic carbon method. The values obtained were used to estimate the mineralization current efficiency according to Eq. (6):

$$MCE(\%) = \frac{(\Delta TOC)_{exp} n F V_s}{4.32 \times 10^7 m I t} \times 100 \tag{6}$$

where $(\Delta TOC)_{exp}$ is the TOC decay at time t, F is the Faraday constant

(96487 C mol^{-1}), V_s is the solution volume (L), 4.32×10^7 is a conversion factor ($= 3600 \, s \, h^{-1} \times 12{,}000 \, mg \, of \, C \, mol^{-1}$), m is the number of carbon atoms of PCM (8 C atoms), I is the applied current (A) and n is the number of electron consumed per molecule of PCM; taken to be 34 assuming complete mineralization of PCM into CO_2, NH_4^+ and H_2O according to Eq. (7).

$$C_8H_9NO_2 + 14H_2O \rightarrow 8CO_2 + NH_4^+ + 33H^+ + 34e^- \qquad (7)$$

The decay kinetics of PCM was followed by injecting 20 µL aliquots to the reversed-phase high performance liquid chromatography (HPLC) (Dionex) equipped with P680 HPLC pump and fitted with a Purosher RP-18, 5 µm, 25 cm × 4.6 mm (i.d.) column at 40 °C. Detection was done with a UVD340U photodiode array detector selected at λ = 254 nm. Isocratic solvent mixture of methanol/phosphate buffer 25:75 (v/v) was used as mobile phase at a flow rate of 0.5 mL min^{-1}. Generated carboxylic acids were detected and quantified by ion-exclusion HPLC using Merck Lachrom liquid chromatograph equipped with an L-2130 pump, fitted with a 30-cm Supelcogel H column (ϕ = 7.8 mm) at 40 °C, and coupled with a L-2400 UV detector selected at wavelength of 210 nm, using 1% H_2SO_4 at 0.2 mL min^{-1} as mobile phase. The inorganic ions majorly NH_4^+ and NO_3^- released in the treated solutions as well as active chlorine species were determined by ion-chromatography (ICS-1000, Dionex) coupled with a Dionex DS6 conductivity detector. The NH_4^+ content was assessed with a Dionex CS12A, 25 cm × 4 mm (i.d.) cation column using 9 mM H_2SO_4 as mobile phase at a flow rate of 1.0 mL min^{-1}. To measure the NO_3^-, Cl^- and ClO_3^- concentrations, a Dionex AS4A-SC, 25 cm × 4 mm (i.d.) anion-exchange column was used with circulation of 1.8 mM Na_2CO_3 and 1.7 mM $NaHCO_3$ solution at 2.0 mL min^{-1} as mobile phase. The concentration of ClO^- was determined by UV/Vis spectrophotometer at 292 nm and correlated with Cl^- because its peak overlap with that of Cl^- in IC chromatograph [41,42].

Aromatic intermediates formed after 60 min of EF treatment of 0.2 mM PCM solutions at 60 mA were identified by GC–MS. The analyses were performed on a Trace 1300 gas chromatograph (Thermo scientific) coupled to a Single Quadrupole ISQ mass spectrophotometer according to method reported elsewhere [20,43].

## 3. Results and discussion

3.1. Degradation kinetics of PCM

The decay of concentration of 30.2 mg L^{-1} (0.2 mM) PCM in 230 mL solutions containing 0.05 M Na_2SO_4, or 0.1 M of either NaCl, $NaNO_3$ or $NaClO_4$ as supporting electrolyte at pH 3.0, comparatively treated by AO-H_2O_2 and EF using either Ti_4O_7, DSA or BDD anode and carbon-felt cathode at applied current of 120 mA was followed by reversed-phased HPLC. PCM displayed a well-defined symmetric peak at a retention time (t_R) of 6.5 min. The degradation efficiency over treatment time was calculated from the following relation:

$$Degradation \, efficiency = \frac{\Delta C_t}{C_0} \times 100 \qquad (8)$$

where ΔC_t is the concentration decay in mg L^{-1} at electrolysis time t (min) and C_o is the corresponding initial concentration (in mg L^{-1}) prior to electrolysis.

Fig. 1 depicts PCM degradation efficiency with specific charge for all the electrolytes studied using different anode materials in either AO-H_2O_2 or EF process. It can be observed that complete degradation (disappearance) of PCM was achieved successfully regardless of the anode material or medium used during both AO-H_2O_2 and EF treatment, indicating the excellent potential of these two EAOPs for effective decontamination of water polluted by PCM. In SO_4^{2-} medium (Fig. 1a), the slowest degradation rate was observed with DSA anode during AO-H_2O_2, which requires over 1 Ah L^{-1} charge for complete disappearance

of PCM in the solution. On the contrary, lower charge (~ 0.5 Ah L^{-1}) was required for complete oxidation of PCM when Ti_4O_7 or BDD anode was used at similar experimental conditions in AO-H_2O_2. The faster degradation observed with both Ti_4O_7 and BDD anodes compared to DSA anode can be explained by the high O_2-evolution over-potential of both Ti_4O_7 and BDD anodes, allowing the production of large quantities of physisorbed Ti_4O_7($^\bullet$OH) or BDD($^\bullet$OH), which led to the effective degradation of the organics compared to DSA($^\bullet$OH). Due to the strong interaction between the anode surface and $^\bullet$OH, the formed radicals at the surface of active anodes like DSA are mainly chemisorbed and behave as relatively weak oxidant compared to physisorbed Ti_4O_7($^\bullet$OH) or BDD($^\bullet$OH). Additionally, there is possibility of production of per-oxidisulfate ($S_2O_8^{2-}$) ions in the sulfate medium [35,44,45] with non-active anodes, especially BDD anode, which is a relatively strong oxidant with longer life-span compared to hydroxyl radicals, thus enhancing the degradation of PCM. The formation of $S_2O_8^{2-}$ from SO_4^{2-} during the electrochemical treatment in sulfate medium especially at high current has been reported by several authors and can simply be explained by Eq. (9) [46]. However, other studies have shown that the formation of $S_2O_8^{2-}$ from SO_4^{2-} is majorly by M($^\bullet$OH)/$^\bullet$OH oxidation of the latter as shown in Eq. (10) [47]. In this case, part of the M($^\bullet$OH)/$^\bullet$OH produced at the surface of BDD/Ti_4O_7 anodes and in the bulk are trapped by an oxidizable species like sulfate to form the corresponding peroxides. At the end, several oxidizing agents could be involved in the mediated oxidizing process because the decomposition of peroxidisulfate gives hydrogen peroxide and other oxidants [44].

$$2SO_4^{2-} \rightarrow S_2O_8^{2-} + 2e^- \qquad (9)$$

$$2HSO_4^- + 2^\bullet OH \rightarrow S_2O_8^{2-} + 2H_2O \qquad (10)$$
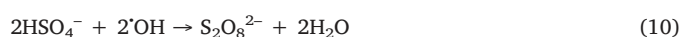
As shown in Fig. 1a, faster degradation of PCM was observed with EF compared to AO-H_2O_2 in all media studied. This is expected because of large quantities of homogeneous $^\bullet$OH produced in the bulk of the solution from Fenton's reaction (Eq. (2)). Thus PCM molecules are destroyed both in bulk of solution by homogeneous $^\bullet$OH and at surface of anode by heterogeneous M($^\bullet$OH) allowing quick oxidation of PCM.

Degradation efficiency results obtained with typical inert anions such as NO_3^- and ClO_4^- (Fig. 1b and 1c respectively) were quite similar and inferior to those obtained in SO_4^{2-} for each electrode under analogous experimental conditions. For instance, complete degradation of PCM was achieved after 2 Ah L^{-1} of applied charge under AO-H_2O_2 condition in either of NO_3^- or ClO_4^- electrolyte with DSA, Ti_4O_7 or BDD anode compared to 1 Ah L^{-1} required in SO_4^{2-} for Ti_4O_7 and BDD anodes. Since the electrolyses were performed in an inert electrolyte, the faster degradation efficiency observed with BDD anode compared to Ti_4O_7 and DSA anodes showed the superior potential of the former for the production of large quantities of BDD($^\bullet$OH). Additionally the slower degradation of PCM observed in these inert electrolytes (NO_3^- and ClO_4^-) compared to sulfate electrolyte during AO-H_2O_2 suggest the formation and participation of $S_2O_8^{2-}$ and sulfate radicals as a weak oxidants in degradation of the pharmaceutical in sulfate medium. As expected, faster degradation was observed under EF treatment condition compared to AO-H_2O_2 in either NO_3^- or ClO_4^- medium with complete removal of PCM attained just after 0.52 Ah L^{-1} of charge with all anode materials. Again in EF, removal efficiency of PCM was much better in sulfate medium compared to either NO_3^- or ClO_4^-, indicating that sulfate is a much better supporting electrolyte in electrochemical wastewater treatment.

In contrast, electrolyses in Cl^- medium (Fig. 1d) exhibited different behavior with both AO-H_2O_2 and EF oxidation, achieving complete degradation of PCM within the first 0.52 and 0.35 Ah L^{-1} of applied charge, respectively, owing to the high contribution of active chlorine species generated from Eqs. (3–5) in the cell, to the overall oxidation of PCM. In both cases of AO-H_2O_2 and EF, faster degradation of PCM was observed in Cl^- medium compared to the other active electrolyte (SO_4^{2-}) or inert medium like NO_3^- and ClO_4^-. The advantage of
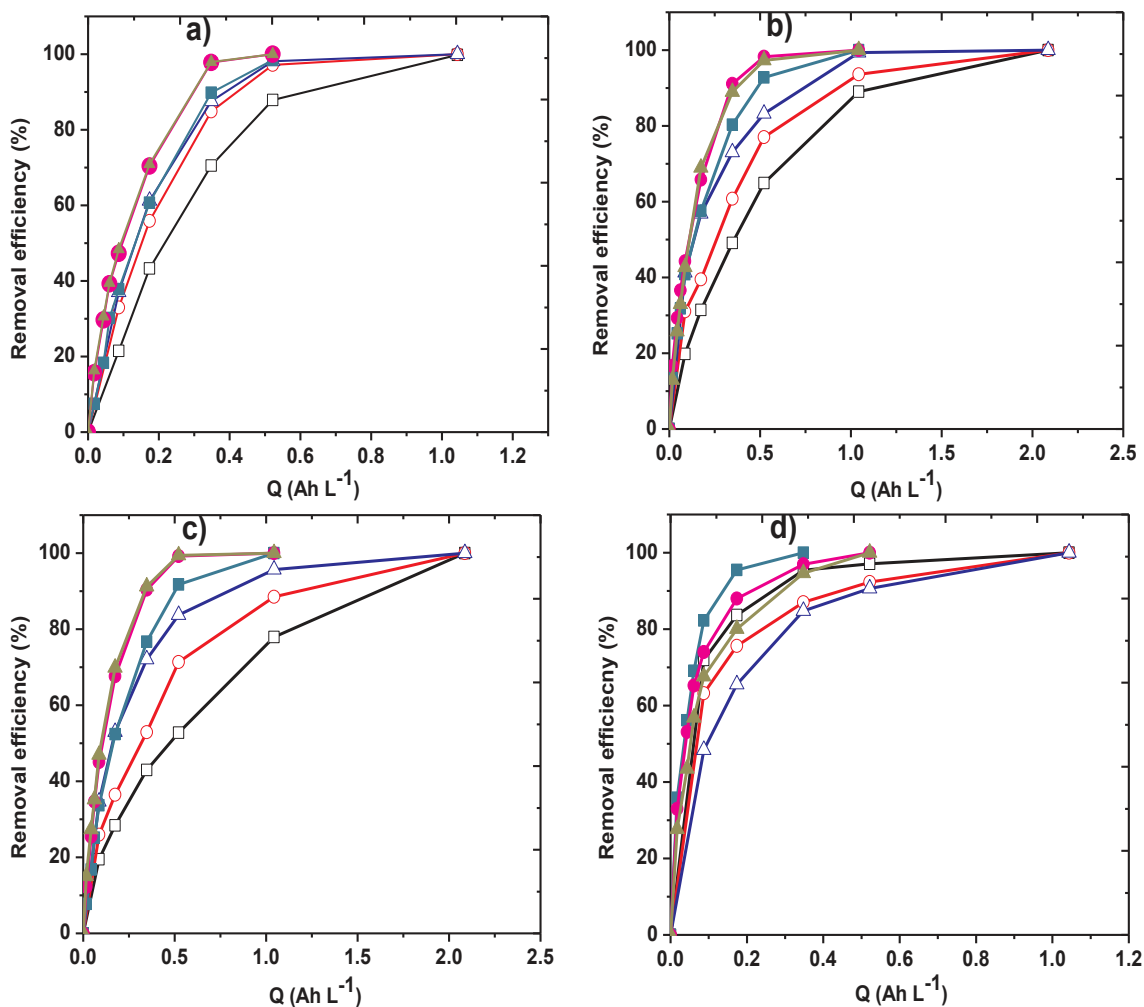
Fig. 1. Removal efficiency vs specific charge for the degradation of 230 mL of 30.2 mg L^{-1} (0.2 mM) PCM solutions in (a) 0.05 M Na$_2$SO$_4$, (b) 0.1 M NaNO$_3$, (c) 0.1 M NaClO$_4$ and (d) 0.1 M NaCl at 120 mA and pH 3. Treatment: (□) AO – DSA, (○) AO – Ti$_4$O$_7$, (△) AO – BDD, (■) EF – DSA, (●) EF – Ti$_4$O$_7$ and (▲) EF – BDD.

electrochemical degradation of organics in Cl$^-$ over SO$_4^{2-}$ medium has been previously observed is several studies. For example, Malpass et al. [11] reported significant mineralization rate of atrazine in NaCl electrolyte using DSA anode owing to production of ClO$^-$ as an active chlorine species, whereas negligible TOC removal were observed with other electrolytes like Na$_2$SO$_4$, NaOH, NaClO$_4$ or NaNO$_3$. Excellent degradation efficiency was also reported for electrooxidation of 17β-estradiol (E2) using BDD anode with complete degradation of 500 μg dm^{-3} E2 attained after 5 min of electrolysis in NaCl compared to 40 min required in Na$_2$SO$_4$ at current density of 25 mA cm^{-2} [44]. Other authors have also shown the benefits of Cl$^-$ over SO$_4^{2-}$ for AO-H$_2$O$_2$ degradation of azo dyes Ponceau 4R [41], reactive red 141, Direct Black 22 and Disperse Orange 29 [48] with BDD anode. Contrary to the results obtained in other media, much better removal efficiency was obtained with DSA compared to Ti$_4$O$_7$ and BDD anodes in Cl$^-$ medium, both during AO-H$_2$O$_2$ and EF treatment (Fig. 1d), owing to its high potential for the production of active chlorine species. Indeed, DSA anode has been shown to be more efficient electrode for the production of active chlorine species compared to non-active anode like BDD [5]. Furthermore, Bagastyo et al. [49] reported formation of more quantities of active chlorine species with DSA anode compared to BDD anodes during the electrochemical oxidation of reverse osmosis concentrate in 0.05 M NaCl. As such, the faster removal efficiency of PCM observed with DSA anode compared to Ti$_4$O$_7$ or BDD anode during the electrolysis in Cl$^-$ medium in this study can be explained by the formation of more active chlorine species with this anode. Moreover, the slower

degradation rate observed with Ti$_4$O$_7$ and BDD could be attributed to scavenging action of Cl$^-$, which consumed the generated Ti$_4$O$_7$/BDD (˙OH) and thus slowing the oxidation reaction.

The effect of current on the degradation efficiency of PCM during treatment with AO-H$_2$O$_2$ and EF using Ti$_4$O$_7$ anode can be seen in Fig. 2. Complete degradation of PCM solution was achieved at all current studied regardless of electrochemical process applied, while lower amounts of charges were consumed at lower current (Fig. 2a). As expected, an increase in current enhanced the removal efficiency of PCM with electrolysis time (Fig. 2b), thanks to the concomitant production of more quantities of hydroxyl radicals at the surface of the anode (AO-H$_2$O$_2$) and in the bulk (EF) (owing to more charge supplied) which can quickly oxidize PCM molecules. Moreover, faster degradation was achieved by EF compared to AO-H$_2$O$_2$ at all current studied, indicating the superiority of EF compared to AO-H$_2$O$_2$ at similar experimental conditions.

3.2. Mineralization (TOC removal) efficiency of PCM solutions

Fig. 3 showed the corresponding TOC removal efficiency with applied charge for all the trial shown in Fig. 1. While complete oxidation of PCM was achieved in all trials, mixed results were obtained for mineralization of the solutions. Poor mineralization of PCM solutions were observed in all AO-H$_2$O$_2$ treatment with DSA anode regardless of the supporting electrolyte media, whereas relative good or excellent mineralization of the solutions was obtained with Ti$_4$O$_7$ and BDD anodes
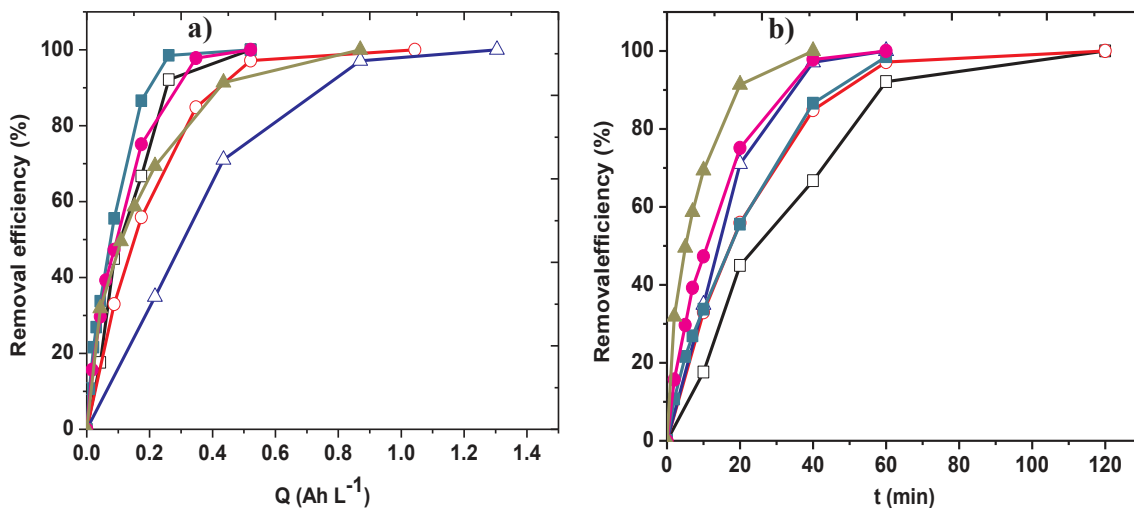
Fig. 2. Effect of current on oxidative degradation efficiency vs (a) charge supplied and (b) electrolysis time for the degradation of 230 mL of 30.2 mg L^{-1} (0.2 mM) PCM solutions in 0.05 M Na$_2$SO$_4$ at pH 3 using Ti$_4$O$_7$ anode. Treatment: (□) AO – 60 mA, (○) AO – 120 mA, (△) AO – 300 mA, (■) EF – 60 mA, (●) EF – 120 mA and (▲) EF – 300 mA.
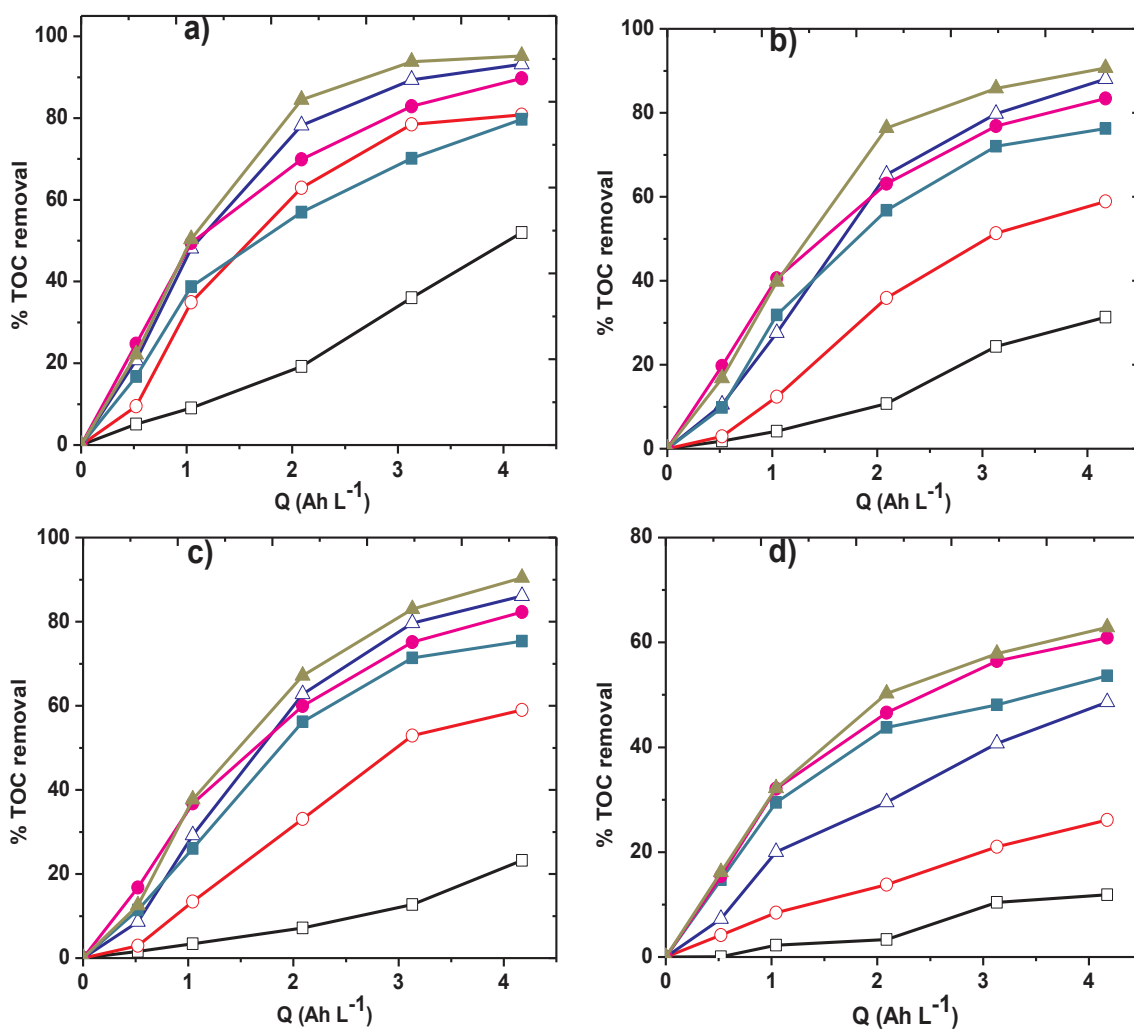

Fig. 3. TOC removal efficiency vs electrolysis time for the mineralization of 230 mL of 30.2 mg L^{-1} (19.2 mg L^{-1} TOC) PCM solutions in (a) 0.05 M Na$_2$SO$_4$, (b) 0.1 M NaNO$_3$, (c) 0.1 M NaClO$_4$ and (d) 0.1 M NaCl at 120 mA constant current intensity and pH 3. Treatment: (□) AO – DSA, (○) AO – Ti$_4$O$_7$, (△) AO – BDD, (■) EF – DSA, (●) EF – Ti$_4$O$_7$ and (▲) EF – BDD.
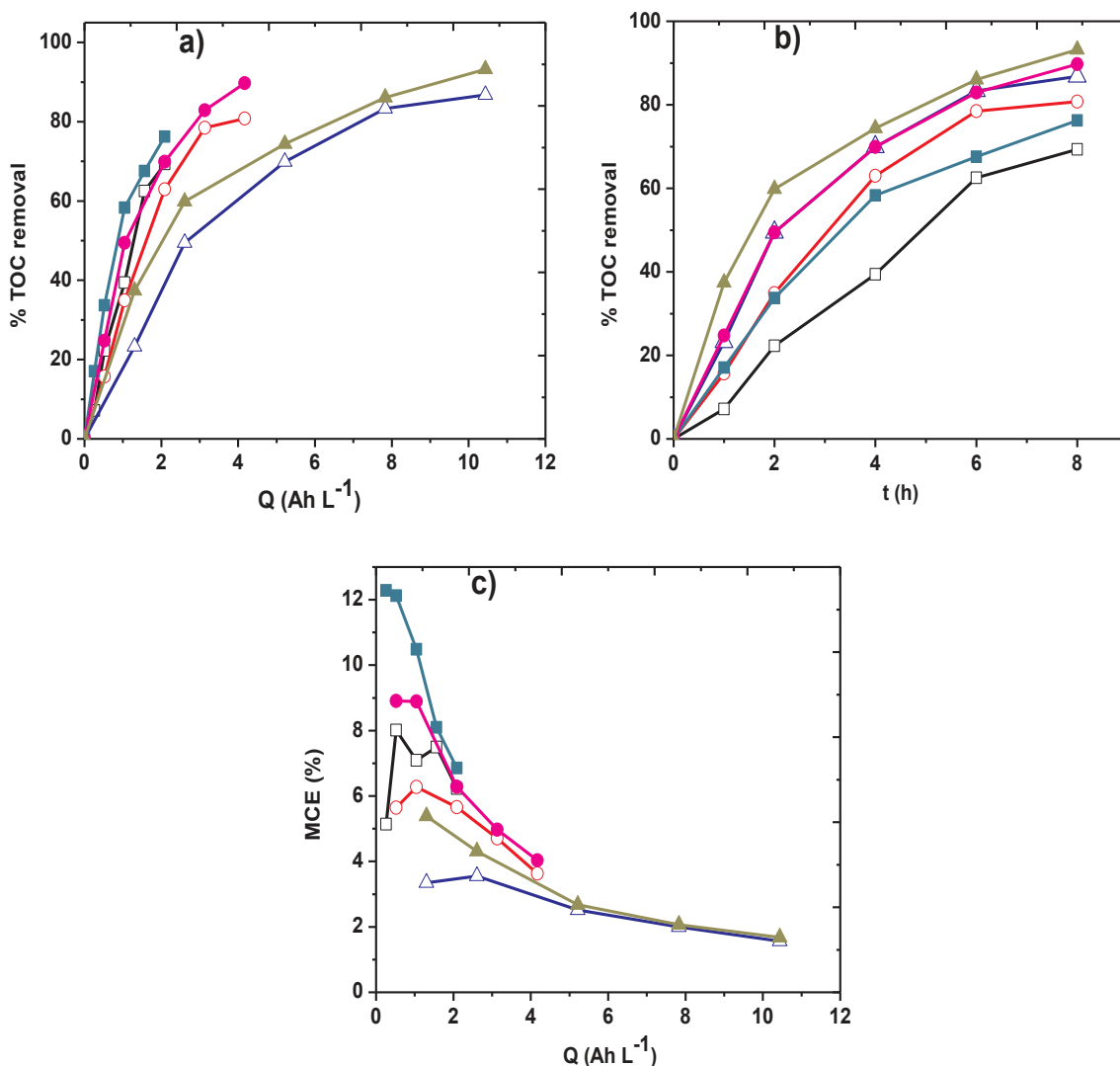
Fig. 4. Effect of applied current vs (a) charge and (b) electrolysis time on TOC removal efficiency and (c) corresponding mineralization current efficiency vs charge, obtained during the mineralization of 230 mL of 30.2 mg L^{-1} (19.2 mg L^{-1} TOC) PCM solutions in 0.05 M Na$_2$SO$_4$ at pH 3 using Ti$_4$O$_7$ anode. Treatments: (□) AO – 60 mA, (O) AO – 120 mA, (△) AO – 300 mA, (■) EF – 60 mA, (●) EF – 120 mA and (▲) EF – 300 mA.

during the AO-H$_2$O$_2$ and EF treatments. The mineralization efficiency for trials in SO$_4^{2-}$ with different anode materials is shown in Fig. 3a. Firstly, it can be seen that for each anode material, EF treatment leads to faster and higher TOC removal efficiency compared to corresponding AO-H$_2$O$_2$ experiments. As explained in Section 3.1, this was attributed to concomitant generations of hydroxyl radicals both at the surface of the anode and in the bulk, as well as reduced diffusion distance between the pollutant and the ˙OH produced in the bulk. As such, in all electrolyte media studied, the mineralization efficiency approximately follows this order: AO-H$_2$O$_2$ – DSA < AO-H$_2$O$_2$ – Ti$_4$O$_7$ < EF – DSA < EF – Ti$_4$O$_7$ ≤ AO-H$_2$O$_2$ – BDD < EF – BDD. The poor and slow TOC removal efficiency achieved in AO-H$_2$O$_2$ with DSA (~50% after 4.17 Ah L^{-1} at 8 h) is due to its low oxidation power, since DSA(˙OH) generated at its surface is readily converted to chemisorbed species which is much less reactive and can only achieve degradation of parent molecule without destroying efficiently the intermediate byproducts [5]. Upon substituting DSA with either Ti$_4$O$_7$ or BDD in AO-H$_2$O$_2$, a remarkable acceleration in TOC removal was achieved with excellent mineralization efficiency up to 81% and 93%, respectively, obtained after 4.17 Ah L^{-1} charges (8 h of electrolysis). Such enhancement can be explained by the greater ability of high oxidation power anodes such as Ti$_4$O$_7$ or BDD to produce loosely adsorbed Ti$_4$O$_7$(˙OH)/BDD(˙OH)

which are powerful oxidants that can easily mineralize both PCM and its organic intermediates compared to a low oxidation power anode like DSA [4,50,51]. On the other hand, EF treatment with DSA attained much better mineralization efficiency (79% after 4.17 Ah L^{-1} charge) compared to AO-H$_2$O$_2$, thanks to the production of large quantities of ˙OH in the bulk from Fenton's reaction (Eq. (2). The homogeneous ˙OH effectively oxidize both PCM and its primary intermediates but less effective in mineralization of refractory final by-products, which accounts for the large residual TOC content (~21%) in the final solution after treatment. Besides, almost complete mineralization (90 and 95% after 4.17 Ah L^{-1} charges) was attained with Ti$_4$O$_7$ and BDD, respectively, during EF, suggesting a beneficial effect of these anodes for the destruction of refractory organic by-products such as carboxylic acids. Indeed, studies have shown that physisorbed hydroxyl radicals (M(˙OH) such as Ti$_4$O$_7$(˙OH) or BDD(˙OH) are more effective than free ˙OH produced in the bulk in mineralization of short-chain carboxylic acids or their complexes with ferric iron ions, which are usually the final end-products in EF treatment [52,53].

The mineralization efficiency results obtained for treatment in ClO$_4^{2-}$ and NO$_3^-$ were quite similar as shown in Fig. 3b and 3c, but slightly lower compared to what was obtained in SO$_4^{2-}$ medium in agreement with degradation efficiency results. As explained in Section
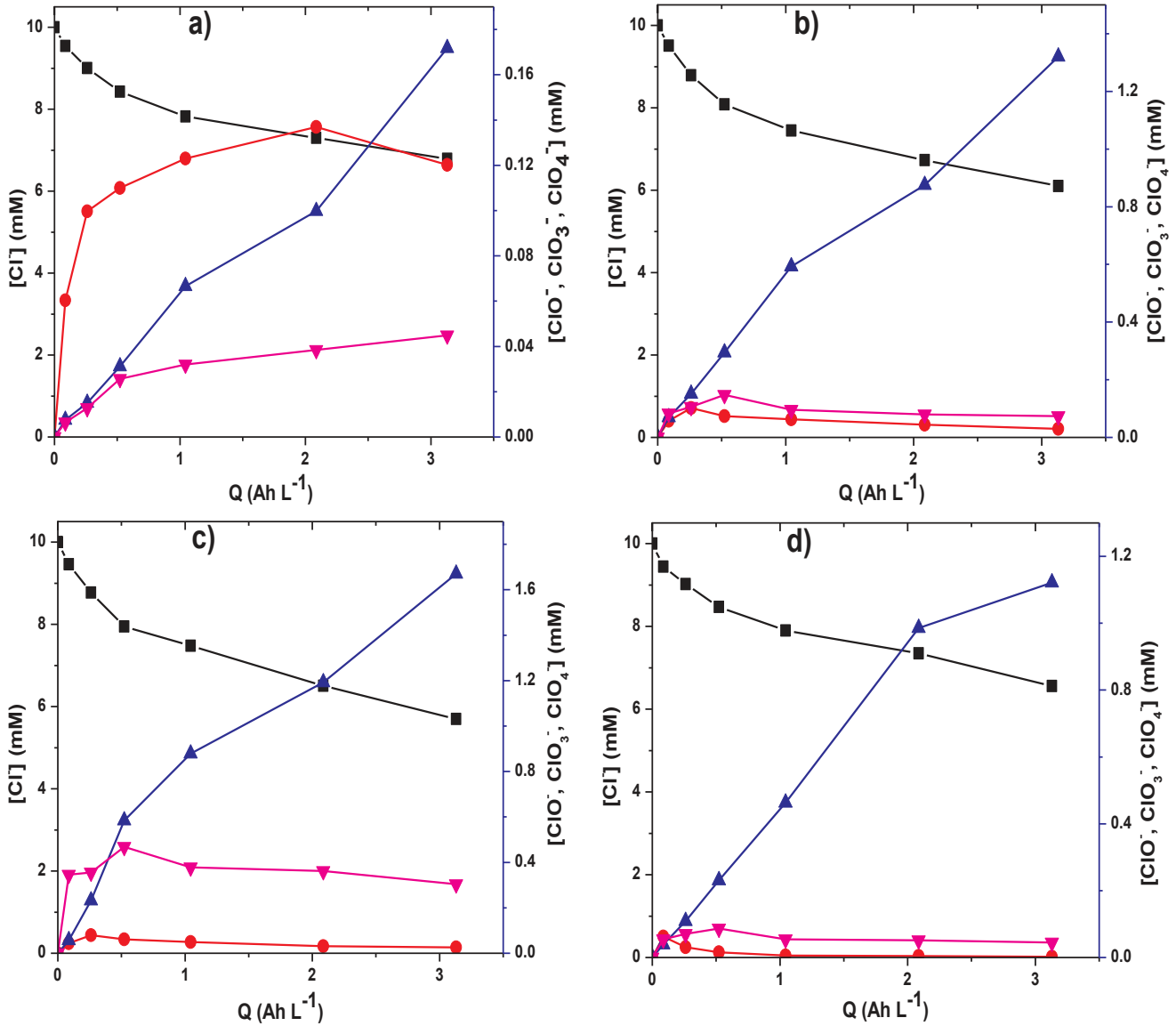
Fig. 5. Evolution of chlorinated ions: (■) Cl^-, (●) ClO^-, (▲) ClO_3^- and (▼) ClO_4^- accumulated during the electrolysis of 230 mL of 10 mM NaCl at pH 3 and 120 mA using (a) AO – DSA, (b) AO – T_4O_7, (c) AO – BDD and (d) EF – Ti_4O_7.

3.1, the slight enhancement of mineralization efficiency observed in SO_4^{2-} compared to ClO_4^- and NO_3^- confirmed the contribution of $S_2O_8^{2-}$ and sulfate radicals formed in SO_4^{2-} medium to the mineralization of PCM and its organic intermediates. In contrast to the faster PCM concentration decay found in Cl^- medium (Section 3.1), a detrimental effect on mineralization efficiency was observed compared to other media (Fig. 3d). In Cl^- medium, a very poor mineralization was observed with all anode materials in AO-H_2O_2 with final TOC removal efficiency of 11%, 27% and 49%, respectively, for DSA, Ti_4O_7 and BDD anodes. The poor TOC removal efficiency can be explained by the partial consumption of heterogeneous hydroxyl radicals by Cl^- to produce less oxidizing species (Eq. (11)).

$$M(^•OH) + Cl^- \rightarrow M + 1/2\ Cl_2 + OH^- \qquad (11)$$

$$H_2O_2 + HClO \rightarrow Cl^- + O_{2(g)} + H_2O + H^+ \qquad (12)$$
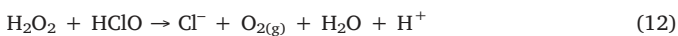
Moreover, slightly better mineralization efficiency was attained in EF treatment with the TOC removal efficiency roses to 53%, 61% and 63% for DSA, Ti_4O_7 and BDD anodes, respectively. Again, after 4.17 Ah L^{-1} charges (8 h of electrolysis) in EF treatment, the TOC removal efficiency in Cl^- was significantly lower (53%–63%) compared to other media

(76%–95%). This behavior can be attributed to four phenomena: (i) the scavenging effect of Cl^- (Eq. (11)) which reduces the contribution of physisorbed radicals to the mineralization of organics, (ii) destruction of the electrogenerated H_2O_2 by active chlorine species (Eq. (12)) which attenuate the Fenton's reaction (Eq. (2)), (iii) depletion of Fe^{2+} in the bulk due to formation of Fe(III)-carboxylic acid complexes and (iv) formation of highly refractory chloro-derivatives [41,54].

The effect of applied current on TOC removal efficiency vs charge for trial conducted in SO_4^{2-} medium using Ti_4O_7 anode is shown in Fig. 4a. As can be observed, enhanced TOC removal efficiency was observed with increased charge consumed (i.e. high current) in both AO-H_2O_2 and EF processes. For instance, the TOC removal efficiency after 8 h of electrolysis at 2.1, 4.2 and 10.4 Ah L^{-1} charges consumed (i.e. 60, 120 and 300 mA) under AO-H_2O_2 condition was 69%, 81% and 89%, respectively, indicating progressive improvement in mineralization efficiency with rise in current. Similar trend was observed in EF treatment with TOC removal efficiency attained 77%, 90% and 94% at 2.1, 4.2 and 10.4 Ah L^{-1} charges consumed, respectively. This is more explicit in Fig. 4b (TOC removal vs electrolysis time) as higher current always led to better TOC removal at all electrolysis time during both AO-H_2O_2 and EF treatment. The greater amount of $Ti_4O_7(^•OH)$
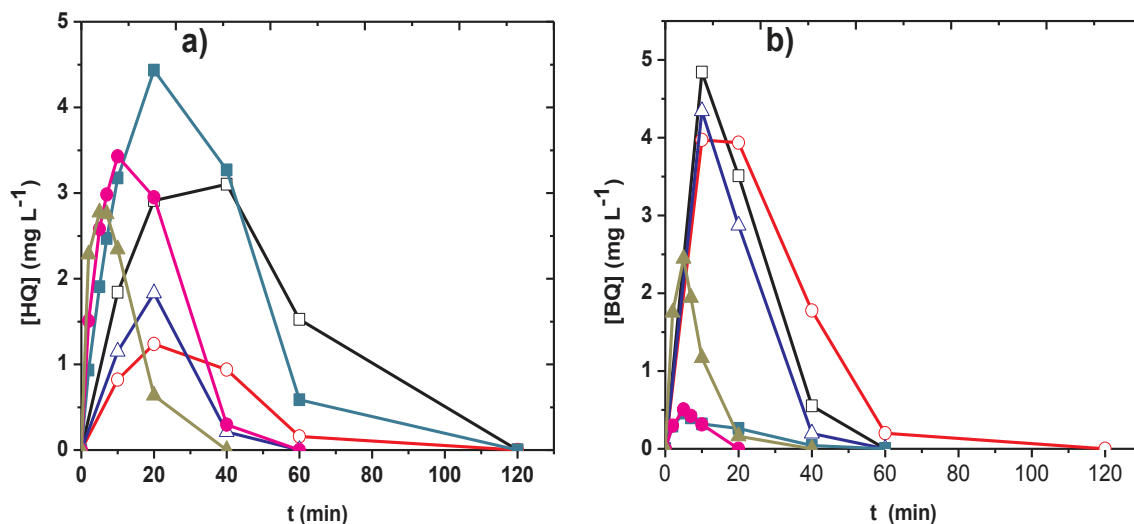
Fig. 6. Evolution of main aromatic intermediates (a) hydroquinone (HQ) and (b) benzoquinone (BQ) during the degradation of 230 mL of 30.2 mg L^{-1} (0.2 mM) PCM solutions in 0.05 M Na$_2$SO$_4$ at pH 3 using Ti$_4$O$_7$ anode. Treatment: (□) AO – 60 mA, (○) AO – 120 mA, (△) AO – 300 mA, (■) EF – 60 mA, (●) EF – 120 mA and (▲) EF – 300 mA.
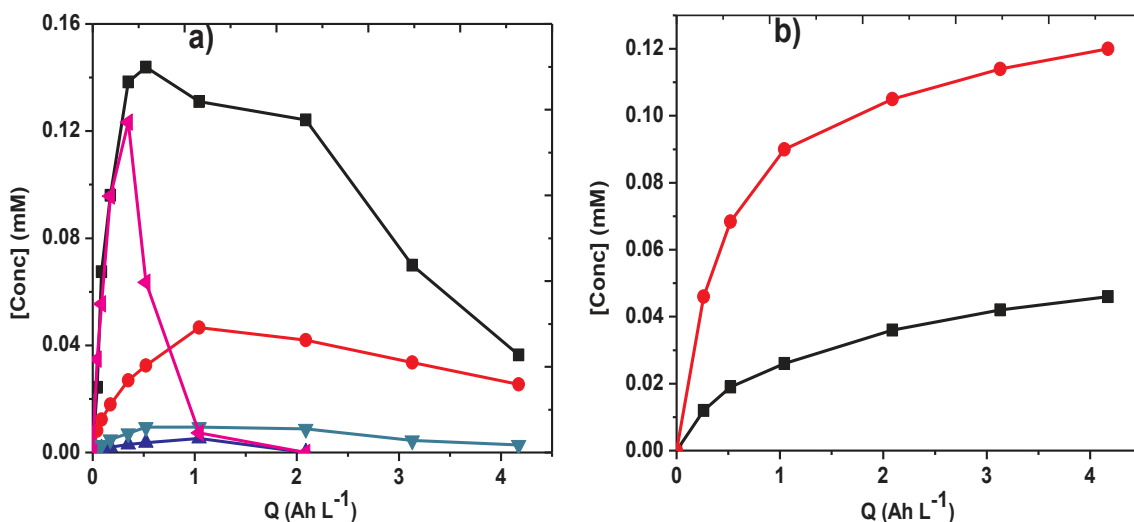

Fig. 7. (a) Evolution of short-chain carboxylic acids: (■) oxalic, (●) oxamic, (▲) maleic, (▼) acetic and (◄) glycoxylic and (b) inorganic ions: (●) NH$_4^+$ and (■) NO$_3^-$ during the mineralization of 230 mL of 30.2 mg L^{-1} (19.2 mg L^{-1} TOC) PCM solutions in 0.05 M Na$_2$SO$_4$ at pH 3 and applied current of 120 mA using Ti$_4$O$_7$ anode.

produced from anodic oxidation of water and the faster electrogeneration of H$_2$O$_2$ and regeneration of Fe^{2+} at higher current accounted for such acceleration of TOC removal [43,55]. However, the enhancement attained when increasing the current from 120 to 300 mA was less remarkable compared to that observed when increasing from 60 to 120 mA (Fig. 4b), suggesting reduction in oxidation ability of the processes due to progressive enhancement of parasitic reactions that consume the generated hydroxyl radicals without contributing efficiently to the mineralization of organics [56]. The mineralization current efficiency (MCE) obtained for each trial of Fig. 4a is given in Fig. 4c. As can be observed, a lower applied current led to a higher MCE at any time compared to higher current, which means that the ratio of organic pollutants to the generated hydroxyl radicals was very high at lower current, thus promoting the oxidation of organics and reducing the effect of parasitic reactions or the self-destruction of the oxidant species.

3.3. Evolution of active chlorine species

The evolution of chlorinated ions during the application of AO-H$_2$O$_2$ and EF in the presence of Cl$^-$ ion was investigated. Typical trials were conducted with a solution containing 10 mM NaCl at pH 3 and 120 mA current using DSA, Ti$_4$O$_7$ or BDD anode with 0.1 mM Fe^{2+} in the case of EF process. As can been seen in Fig. 5, Cl$^-$ ion was gradually disappearing from the solution via direct electrochemical oxidation (Eq. (3)) and M($\cdot$OH)/$\cdot$OH destruction (Eq. (11)) at the anode and in the bulk, whereas ClO$^-$ is significantly more accumulated with DSA anode (Fig. 5a) compared to Ti$_4$O$_7$ (Fig. 5b) or BDD (Fig. 5c) anodes. This can be attributed to higher oxidation power of Ti$_4$O$_7$ and BDD anode in which ClO$^-$ is quickly oxidized to ClO$_3^-$ and ClO$_4^-$ (Fig. 5b and c). It is important to state that ClO$_3^-$ is the highest accumulated chlorine species in all case with quite similar and higher concentration (1–1.6 mM) for Ti$_4$O$_7$ and BDD anodes, whereas much lower quantities (0.17 mM) was attained with DSA anode. Again, ClO$_4^-$ was more accumulated with BDD than Ti$_4$O$_7$, whereas its accumulation is lowest with DSA anode. Interestingly accumulation-destruction profiles were
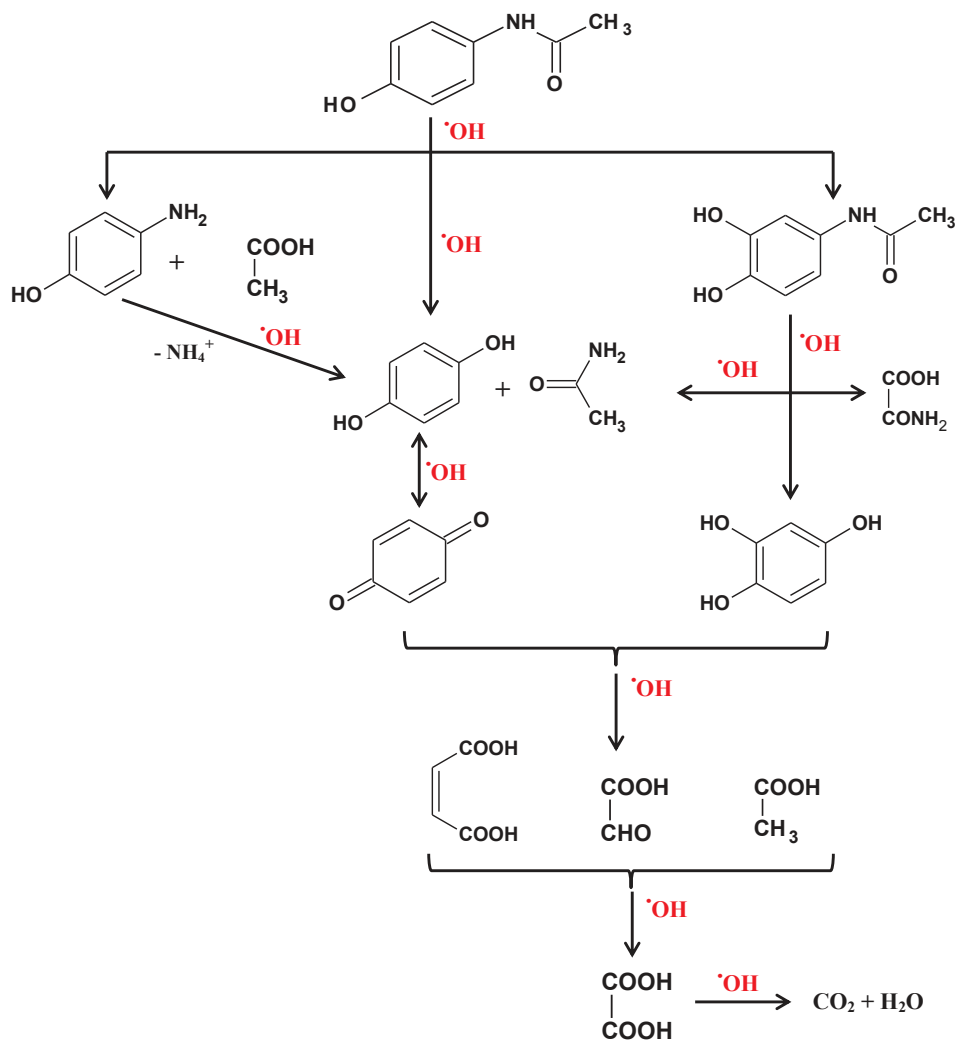
Fig. 8. Proposed reaction pathways based on identified by-products for complete mineralization of PCM by hydroxyl radicals.

obtained for ClO^- and ClO_4^- with both Ti_4O_7 and BDD anodes, whereas continuous accumulation with plateau was observed with DSA anode. The higher ClO^- observed with DSA anode (Fig. 5a) could explain the faster degradation of PCM obtained with DSA anode compared to Ti_4O_7 and BDD anodes in Cl^- medium as reported in Fig. 1d, since ClO^- is a better oxidant compared to ClO_3^- and ClO_4^-. Moreover, similar trend was observed during EF oxidation with Ti_4O_7 anode (Fig. 5d) however, with lower accumulation of ClO^-, ClO_3^- and ClO_4^- and slower decay of Cl^- compared to $AO-H_2O_2$ with the same anode. The lower quantity of ClO^- observed in all cases could be as a result of the initial pH of the solutions (pH ~ 3) since HClO formation rather than ClO^- is favored at strong acidic pH.

3.4. Evolution of oxidation by-products and reaction pathways

The kinetics and mineralization studies previously discussed have been accompanied by the identification of aromatic intermediates, carboxylic acids and inorganic ions. Two cyclic/aromatic intermediates were detected and quantified during the degradation of PCM. Based on previous study [36,37] and by injecting standard solutions in reversed phase HPLC using similar conditions as that of PCM, the two intermediates were confirmed to be hydroquinone (t_R = 5.2 min) and benzoquinone (t_R = 9.5 min) and their evolution with time are shown in Fig. 6a and 6b. It can be seen that the by-products are formed right from the beginning of electrolyses, which corresponds to the oxidation of PCM. In all trials, a typical accumulation-destruction cycle was

observed for both intermediate products at all currents studied, thanks to greater formation from the PCM destruction at the early stage of electrolysis, followed by the predominant oxidation/degradation by the large quantities of hydroxyl radicals generated as treatment time increases. As in the case of PCM oxidation (Fig. 2), the degradation rate of both byproducts increased when the applied current was raised, thus complete disappearance of both byproducts was achieved in very short time at the highest current in both $AO-H_2O_2$ and EF treatment. Maximum concentration of 4.8 mg L^{-1} and 4.4 mg L^{-1} were attained for hydroquinone and benzoquinone, respectively. It is important to note that hydroquinone was more accumulated in $AO-H_2O_2$, whereas the formation of benzoquinone was prominent during EF treatment.

Further degradation of these aromatic by-products yielded several short-chain carboxylic acids as shown by ion-exclusion HPLC analysis. The chromatograms always showed the presence of oxalic acid (t_R = 8.6 min), maleic acid (t_R = 10.6 min), oxamic acid (t_R = 12.7 min), acetic acid (t_R = 14.2 min) and glyoxylic acid (t_R = 17.1 min), mostly formed at the early stage of the electrolysis. As shown in Fig. 7a, a cycle of accumulation –destruction was observed, thanks to the faster transformation of the primary aromatics intermediates into short-chain carboxylic acids at early stage, and destruction at much longer treatment time. Oxalic acid was the most persistent and highest accumulated with maximum concentration of 0.14 mM in agreement with previous reports [52,53]. The presence of non-mineralized carboxylic acids after 4.17 Ah L^{-1} (8 h of electrolysis) as presented in Fig. 7a can be accounted for the residual TOC (Fig. 4a) of the

final treated solution.

The possible loss of initial nitrogen content of PCM in form of inorganic ions such as NH_4^+, NO_2^- or NO_3^- during its mineralization was followed by ion chromatography. As shown in Fig. 7b, the NH_4^+ ions were predominant along with smaller proportion of NO_3^- without detecting NO_2^-. A rapid accumulation of both NH_4^+ and NO_3^- was observed at the early stage of the treatment, which agrees with the faster destruction of PCM and its primary intermediate products. After 8 h of treatment (4.17 Ah L^{-1}), 0.12 mM NH_4^+ (60% of initial N) and 0.046 mM NO_3^- (23% of initial N) was released into the treated solution. Approximately 0.03 mM of the initial N (15%) was present in the final solution as non-mineralized organic by-products (oxamic acid) (Fig. 7a), while the remaining 2% of the initial N may have been lost as volatile nitrogen compounds [57].

The reaction mechanism for the complete mineralization of PCM by hydroxyl radicals based on the identified intermediates was shown in Fig. 8. Three possible pathways can be identified for the oxidation of primary PCM molecule: (i) N-dealkylation at amine group with formation of aromatic by-product hydroquinone, (ii) hydroxyl radicals attacks on the peptide bond with the formation of 4-amino phenol, and (iii) hydroxylation of paracetamol molecule to 2-hydroxyl-4-(N-acetyl) aminophenol. Further oxidation of both 4-amino phenol and 2-hydroxyl-4-(N-acetyl) aminophenol could lead to the formation of hydroquinone with the release of NH_4^+, acetamide and acetic acid. Oxidation of 2-hydroxyl-4-(N-acetyl) aminophenol could also proceed via dealkylation at amine group with formation of 1,2,4-trihydroxyl benzene, which was identified by GC–MS. Similar oxidation products have been previously reported for the degradation of PCM by O_3, H_2O_2/UVA and Fe^{3+} + Cu^{2+}/O_3/UVA as well as EF using platinum electrode, with the ˙OH oxidation of PCM leading to the formation of 2-hydroxyl-4-(N-acetyl) aminophenol and hydroquinone as well as accelerated their degradation into benzoquinone [32,58]. The oxidation of aryl moiety of the aromatic by-products (hydroquinone and benzoquinone) gives short-chain carboxylic acids such as oxalic, maleic and glycoxylic acids, whereas oxamic acid was formed either from the degradation of 2-hydroxyl-4-(N-acetyl) aminophenol or oxidation of acetamide. Oxalic acid may also be generated from further degradation of maleic and glycoxylic acids. All the carboxylic acids were further mineralized to CO_2 and H_2O by hydroxyl radicals accompanied with the release of NH_4^+/ NO_3^-.

4. Conclusions

The efficiency of ceramic Ti_4O_7 anode for the treatment of acidic solution of PCM by AO-H_2O_2 and EF oxidation in different electrolytes has been investigated. The PCM removal efficiency was much quick in Cl^- compared SO_4^{2-} medium, which in turn faster than in both NO_3^- and ClO_4^-, thanks to the generation of secondary oxidants like active chlorine species and peroxidisulfate ions in Cl^- and SO_4^{2-}, respectively. On the contrary, the mineralization of PCM solution was in the order: $Cl^- \ll ClO_4^- \approx NO_3^- < SO_4^{2-}$ medium. In all electrolytes, the mineralization efficiency for the treatment of PCM solutions approximately increased in the order: AO-H_2O_2–DSA < AO-H_2O_2–Ti_4O_7 < EF–DSA < EF–Ti_4O_7 ≈ AO-H_2O_2–BDD < EF–BDD. The Ti_4O_7 anode was found to be more efficient for ClO^- generation compared to BDD but inferior to DSA. The mineralization of PCM proceeds via the formation of aromatic by products – hydroquinone and benzoquinone, which were further degraded to several carboxylic acids before final mineralization to CO_2 and water. The Ti_4O_7 anode has shown to be an efficient anode material for quick electrochemical oxidation and excellent mineralization of PCM in SO_4^{2-}, NO_3^- or ClO_4^- medium but less efficient in Cl^- medium.

Acknowledgement

Appendix A. Supplementary material

Supplementary data associated with this article can be found, in the online version, at https://doi.org/10.1016/j.seppur.2018.03.076.

References

[1] E. Brillas, I. Sirés, M.A. Oturan, Electro-Fenton process and related electrochemical technologies based on Fenton's reaction chemistry, Chem. Rev. 109 (2009) 6570–6631.

[2] M.A. Rodrigo, N. Oturan, M.A. Oturan, Electrochemically assisted remediation of pesticides in soils and water: a review, Chem. Rev. 114 (2014) 8720–8745.

[3] C.A. Martínez-Huitle, M.A. Rodrigo, I. Sirés, O. Scialdone, Single and coupled electrochemical processes and reactors for the abatement of organic water pollutants: a critical review, Chem. Rev. 115 (2015) 13362–13407.

[4] M.A. Oturan, J.J. Aaron, Advanced oxidation processes in water/wastewater treatment: principles and applications. A review, Crit. Rev. Environ. Sci. Technol. 44 (2014) 2577–2641.

[5] M. Panizza, G. Cerisola, Direct and mediated anodic oxidation of organic pollutants, Chem. Rev. 109 (2009) 6541–6569.

[6] R. Salazar, M.S. Ureta-Zañartu, C. González-Vargas, C.N. Brito, C.A. Martínez-Huitle, Electrochemical degradation of industrial textile dye disperse yellow 3: role of electrocatalytic material and experimental conditions on the catalytic production of oxidants and oxidation pathway, Chemosphere 198 (2018) 21–29.

[7] S.O. Ganiyu, E.D. van Hullebusch, M. Cretin, G. Esposito, M.A. Oturan, Coupling of membrane filtration and advanced oxidation processes for removal of pharmaceutical residues: a critical review, Sep. Purif. Technol. 156 (2015) 891–914.

[8] E. Mousset, N. Oturan, M.A. Oturan, An unprecedented route of •OH radical reactivity evidenced by an electrocatalytical process: ipso-substitution with perhalogenocarbon compounds, Appl. Cat. B: Environ. 226 (2018) 135–146.

[9] E. Mousset, N. Oturan, E.D. van Hullebusch, G. Guibaud, G. Esposito, M.A. Oturan, Treatment of synthetic soil washing solution containing phenanthrene and cyclodextrin by electro-oxidation. Influence of anode material on toxicity removal and biodegradability enhancement, Appl. Cat. B: Environ. 160–161 (2014) 666–675.

[10] E. Mousset, Z. Wang, J. Hammaker, O. Lefebvre, Electrocatalytic phenol degradation by a novel nanostructured carbon fiber brush cathode coated with graphene ink, Electrochim. Acta 258 (2017) 607–617.

[11] G.R.P. Malpass, D.W. Miwa, D.A. Mortari, S.A.S. Machado, A.J. Motheo, Decolorization of real textile waste using electrochemical techniques: effect of the chloride concentration, Water Res. 41 (2007) 2969–2977.

[12] M. Mascia, A. Vacca, A.M. Polcaro, S. Palmas, J.R. Ruiz, A. Da Pozzo, Electrochemical treatment of phenolic waters in presence of chloride with boron-doped diamond (BDD) anodes: experimental study and mathematical model, J. Hazard. Mater. 174 (2010) 314–322.

[13] L. Chen, P. Campo, M.J. Kupferle, Identification of chlorinated oligomers formed during anodic oxidation of phenol in the presence of chloride, J. Hazard. Mater. 283 (2015) 574–581.

[14] A.Y. Bagastyo, D.J. Batstone, I. Kristiana, W. Gernjak, C. Joll, J. Radjenovic, Electrochemical oxidation of reverse osmosis concentrate on boron-doped diamond anodes at circumneutral and acidic pH, Water Res. 46 (2012) 6104–6112.

[15] A. Thiam, R. Salazar, E. Brillas, I. Sirés, Electrochemical advanced oxidation of carbofuran in aqueous sulfate and/or chloride media using a flow cell with a RuO₂-based anode and an air-diffusion cathode at pre-pilot scale, Chem. Eng. J. 335 (2018) 133–144.

[16] B.P. Chaplin, Critical review of electrochemical advanced oxidation processes for water treatment applications, Environ. Sci. Process. Impacts 16 (2014) 1182–1203.

[17] A.M. Zaky, B.P. Chaplin, Mechanism of p-substituted phenol oxidation at a Ti_4O_7 reactive electrochemical membrane, Environ. Sci. Technol. 48 (2014) 5857–5867.

[18] F.C. Walsh, R.G.A. Wills, The continuing development of Magnéli phase titanium sub-oxides and Ebonex® electrodes, Electrochim. Acta 55 (2010) 6342–6351.

[19] D. Bejan, J.D. Malcolm, L. Morrison, N.J. Bunce, Mechanistic investigation of the conductive ceramic Ebonex® as an anode material, Electrochim. Acta 54 (2009) 5548–5556.

[20] S.O. Ganiyu, N. Oturan, S. Raffy, M. Cretin, R. Esmilaire, E. van Hullebusch, G. Esposito, M.A. Oturan, Sub-stoichiometric titanium oxide (Ti_4O_7) as a suitable ceramic anode for electrooxidation of organic pollutants: a case study of kinetics, mineralization and toxicity assessment of amoxicillin, Water Res. 106 (2016) 171–181.

[21] S. You, B. Liu, Y. Gao, Y. Wang, C.Y. Tang, Y. Huang, N. Ren, Monolithic porous Magnéli-phase Ti_4O_7 for electro-oxidation treatment of industrial wastewater, Electrochim. Acta 214 (2016) 326–335.

[22] S.O. Ganiyu, N. Oturan, S. Raffy, G. Esposito, E.D. van Hullebusch, M. Cretin, M.A. Oturan, Use of sub-stoichiometric titanium oxide as a ceramic electrode in anodic oxidation and electro-Fenton degradation of the beta-blocker propranolol: degradation kinetics and mineralization pathway, Electrochim. Acta 242 (2017) 344–354.

[23] R.J. Pollock, J.F. Houlihan, A.N. Bain, B.S. Coryea, Electrochemical properties of a new electrode material, Ti4O7, Mater. Res. Bull. 19 (1984) 17–24.

[24] J.R. Smith, F.C. Walsh, R.L. Clarke, Electrodes based on Magneli phase titanium oxides: the properties and applications of Ebonex(R) materials, J. Appl. Electrochem.

28 (1998) 1021–1033.

[25] J.E. Graves, D. Pletcher, R.L. Clarke, F.C. Walsh, The electrochemistry of Magnéli phase titanium oxide ceramic electrodes Part I. The deposition and properties of metal coatings, J. Appl. Electrochem. 21 (1991) 848–857.

[26] P. Geng, J. Su, C. Miles, C. Comninellis, G. Chen, Highly-ordered Magnéli Ti_4O_7 nanotube arrays as effective anodic material for electro-oxidation, Electrochim. Acta 153 (2015) 316–324.

[27] D. Bejan, E. Guinea, N.J. Bunce, On the nature of the hydroxyl radicals produced at boron-doped diamond and Ebonex® anodes, Electrochim. Acta 69 (2012) 275–281.

[28] N. Oturan, S.O. Ganiyu, S. Raffy, M.A. Oturan, Sub-stoichiometric titanium oxide as a new anode material for electro-Fenton process: application to electrocatalytic destruction of antibiotic amoxicillin, Appl. Catal. B Environ. 217 (2017) 214–223.

[29] T.A. Ternes, Occurrence of drugs in German sewage treatment plants and rivers: dedicated to Professor Dr. Klaus Haberer on the occasion of his 70th birthday, Water Res. 32 (1998) 3245–3260.

[30] D.W. Kolpin, E.T. Furlong, M.T. Meyer, E.M. Thurman, S.D. Zaugg, L.B. Barber, H.T. Buxton, Pharmaceuticals, hormones, and other organic wastewater con- taminants in U.S. streams, 1999–2000: a national reconnaissance, Environ. Sci. Technol. 36 (2002) 1202–1211.

[31] I. Kabdasli, O. Tunay, D. Orhon, Wastewater control and management in a leather tanning district, Water Sci. Technol. 40 (1999) 261–267.

[32] B. Halling-Sørensen, S. Nors Nielsen, P.F. Lanzky, F. Ingerslev, H.C. HoltenLützhøft, S.E. Jørgensen, Occurrence, fate and effects of pharmaceutical substances in the environment: a review, Chemosphere 36 (1998) 357–393.

[33] K. Kümmerer, Drugs in the environment: emission of drugs, diagnostic aids and disinfectants into wastewater by hospitals in relation to other sources – a review, Chemosphere 45 (2001) 957–969.

[34] I.A. Balcioglu, M. Otker, Treatment of pharmaceutical wastewater containing an- tibiotics by O_3 and O_3/H_2O_2 processes, Chemosphere 50 (2003) 85–95.

[35] E. Brillas, I. Sirés, C. Arias, P.L. Cabot, F. Centellas, R.M. Rodríguez, J.A. Garrido, Mineralization of paracetamol in aqueous medium by anodic oxidation with boron- doped diamond electrode, Chemosphere 58 (2005) 399–406.

[36] M. Skoumal, P.L. Cabot, F. Centellas, C. Arias, R.M. Rodríguez, J.A. Garrido, E. Brillas, Mineralization of paracetamol by ozonation catalyzed with Fe^{2+}, Cu^{2+} and UVA light, Appl. Catal. B: Environ. 66 (2006) 228–240.

[37] R. Andreozzi, V. Caprio, R. Marotta, D. Vogna, Paracetamol oxidation from aqueous solutions by means of ozonation and H_2O_2/UV system, Water Res. 37 (2003) 993–1004.

[38] K. Waterston, J.W. Wang, D. Bejan, N.J. Bunce, Electrochemical wastewater treat- ment: electrooxidation of acetaminophen, J. Appl. Electrochem. 36 (2006) 227–232.

[39] I. Sirés, C. Arias, P.L. Cabot, F. Centellas, R.M. Rodríguez, J.A. Garrido, E. Brillas, Paracetamol mineralization by advanced electrochemical oxidation processes for wastewater treatment, Environ. Chem. 1 (2004) 26–28.

[40] T.X.H. Le, C. Charmette, M. Bechelany, M. Cretin, Facile preparation of porous carbon cathode to eliminate paracetamol in aqueous medium using electro-Fenton system, Electrochim. Acta 188 (2016) 378–384.

[41] A. Thiam, E. Brillas, F. Centellas, P.L. Cabot, I. Sirés, Electrochemical reactivity of Ponceau 4R (food additive E124) in different electrolytes and batch cells, Electrochim. Acta 173 (2015) 523–533.

[42] T. Chen, Spectrophotometric determination of microquantities of chlorate, chlorite, hypochlorite and chloride in perchlorate, Anal. Chem. 39 (1967) 804.

[43] A. Dirany, I. Sirés, N. Oturan, A. Özcan, M.A. Oturan, Electrochemical treatment of the antibiotic sulfachloropyridazine: kinetics, reaction pathways, and toxicity evolution, Environ. Sci. Technol. 46 (2012) 4074–4082.

[44] M. Murugananthan, S. Yoshihara, T. Rakuma, N. Uehara, T. Shirakashi, Electrochemical degradation of 17β-estradiol (E2) at boron-doped diamond (Si/ BDD) thin film electrode, Electrochim. Acta 52 (2007) 3242–3249.

[45] P.A. Michaud, M. Panizza, L. Ouattara, T. Diaco, G. Foti, C. Comninellis, Electrochemical oxidation of water on synthetic boron-doped diamond thinfilm anodes, J. Appl. Electrochem. 33 (2003) 151–154.

[46] P. Canizares, C. Saez, J. Lobato, M.A. Rodrigo, Electrochemical oxidation of poly- hydroxybenzenes on boron-doped diamond anodes, Ind. Eng. Chem. Res. 43 (2004) 6629–6637.

[47] M. Panizza, G. Cerisola, Application of diamond electrodes to electrochemical processes, Electrochim. Acta 51 (2005) 191–199.

[48] J.M. Aquino, M.A. Rodrigo, R.C. Rocha-Filho, C. Sáez, P. Cañizares, Influence of supporting electrolytes on the electrolyses of dyes with conductive-diamond an- odes, Chem. Eng. J. 184 (2012) 221–227.

[49] A.Y. Bagastyo, D.J. Batstone, K. Rabaey, J. Radjenovic, Electrooxidation of elec- trodialysed reverse osmosis concentrate on Ti/Pt-IrO₂, Ti/SnO₂-Sb and boron- doped diamond electrodes, Water Res. 47 (2013) 242–250.

[50] I. Sirés, E. Brillas, M.A. Oturan, M.A. Rodrigo, M. Panizza, Electrochemical ad- vanced oxidation processes: today and tomorrow. A review, Environ. Sci. Pollut. Res. 21 (2014) 8336–8367.

[51] M.A. Oturan, Electrochemical advanced oxidation technologies for removal of or- ganic pollutants from water, Environ. Sci. Pollut. Res. 21 (2014) 8333–8335.

[52] M.A. Oturan, M. Pimentel, N. Oturan, I. Sirés, Reaction sequence for the miner- alization of the short-chain carboxylic acids usually formed upon cleavage of aro- matics during electrochemical Fenton treatment, Electrochim. Acta 54 (2008) 173–182.

[53] S. Garcia-Segura, E. Brillas, Mineralization of the recalcitrant oxalic and oxamic acids by electrochemical advanced oxidation processes using a boron-doped dia- mond anode, Water Res. 45 (2011) 2975–2984.

[54] D.C. de Moura, C.K. Costa de Araújo, C.L.P.S. Zanta, R. Salazar, C.A. Martínez- Huitle, Active chlorine species electrogenerated on $Ti/Ru_{0.3}Ti_{0.7}O_2$ surface: elec- trochemical behavior, concentration determination and their application, J. Electroanal. Chem. 731 (2014) 145–152.

[55] N. Oturan, J. Wu, H. Zhang, V.K. Sharma, M.A. Oturan, Electrocatalytic destruction of the antibiotic tetracycline in aqueous medium by electrochemical advanced oxidation processes: effect of electrode materials, Appl. Catal. B: Environ. 140–141 (2013) 92–97.

[56] I. Sirés, N. Oturan, M.A. Oturan, Electrochemical degradation of β-blockers. Studies on single and multicomponent synthetic aqueous solutions, Water Res. 44 (2010) 3109–3120.

[57] S. Garcia-Segura, E. Mostafa, H. Baltruschat, Could NO_x be released during mi- neralization of pollutants containing nitrogen by hydroxyl radical? Ascertaining the release of N-volatile species, Appl. Cat B: Environ. 207 (2017) 376–384.

[58] T.X.H. Le, T.V. Nguyen, Z. Amadou Yacouba, L. Zoungrana, F. Avril, D.L. Nguyen, E. Petit, J. Mendret, V. Bonniol, M. Bechelany, S. Lacour, G. Lesage, M. Cretin, Correlation between degradation pathway and toxicity of acetaminophen and its by-products by using the electro-Fenton process in aqueous media, Chemosphere 172 (2017) 1–9.